Dynamic Characteristics of Externally Pressurized, Double-Pad, Circular Thrust Bearings With Membrane Restrictors

C. Wang

C. Cusano

Department of Mechanical and Industrial Engineering,
University of Illinois at Urbana-Champaign,
Urbana, IL 61801

The dynamic characteristics of externally pressurized, double-pad, circular thrust bearings with membrane variable flow compensation are analytically studied. Under static loads or load composed of a static and cyclic component, membrane compensation gives better overall performance characteristics than capillary (fixed flow) compensation. As the frequency increases, capillary compensation gives approximately the same performance as optimal membrane compensation when the bearing operates under pure cyclic loading.

Introduction

Externally pressurized bearings are widely used in applications such as machine tools, measuring instruments, and testing machines. The performance of these bearings is sensitive to the type of internal compensation. Generally, there are two types of compensation. One is passive compensation, examples of which are capillary and orifice restrictors. The other is active compensation, which includes spools, membranes, and constant-flow-rate valves. For passively compensated bearings, the geometry of the compensating element does not change when the operating conditions are varied. For actively compensated bearings, however, the internal geometrical configuration is automatically adjusted by means of either a load sensing device or a pressure sensing device. Generally, higher load capacity and stiffness are attainable when the bearing is actively compensated.

Since the 1960s, externally pressurized bearings with variable flow restrictors have been investigated by many researchers. For steady-state conditions, contributions to the behavior of these bearings have been made by De Gast (1966), Mayer and Shaw (1963), O'Donoghue and Rowe (1969), and Cusano (1974). Since these bearings often operate under dynamic conditions or subjected to disturbances, their dynamic performance is of interest to designers. However, analyses reported in the literature concerning the dynamic behavior of externally pressurized bearings having fixed or variable-flow restrictors are limited. Among these analyses is that of De Gast (1966) who experimentally studied the response of a membrane compensated bearing subjected to a sinusoidal load. The squeeze film damping of an externally pressurized bearing and its effect on the vibratory response of machinery, particularly machine tools, was investigated by Brown (1961). However, he used a simple linear, spring-damper, massless model and assumed that the supply pressure is equal to the recess pressure of the bearing. Licht and Colley (1964) presented a theoretical analysis on the performance characteristics of externally-pressurized sliders with both incompressible and compressible lubricants. They mainly focused on system stability analysis considering small displacements from the equilibrium gap height. Optiz et al. (1969) analytically studied the dynamic behavior of an externally pressurized spindle bearing with capillary compensation. Since their results are based on an equivalent linear mass-spring-damping system, the validity of the results are limited. Perhaps, the most rigorous analysis of the dynamic characteristics of externally pressurized bearing is due to Ghosh and Majamdar (1982). They studied the stiffness and damping characteristics of externally pressurized thrust bearings by linearizing the governing equations using a first order perturbation method. Although their model contained many features such as effects of fluid inertia and recess volume fluid compressibility, the analysis was limited to passively compensated systems with a capillary or orifice restrictor.

In this paper, the dynamic behavior of an externally pressurized doublepad, circular thrust bearing with membrane compensation is analytically studied. The circular geometry is used for its simplicity. Similar results, however, are expected if other geometries were used. The bearing is modeled as a two-degree-of-freedom nonlinear system. Both the steady state and transient behavior of the bearing, when it is subjected to a static or dynamic load, are analyzed. A wide range of system parameters, such as membrane stiffness, supply pressure, and recess-to-supply pressure ratio, are considered under various loading conditions.

Problem Formulation

The following analysis is based on the assumptions given below:

Contributed by the Tribology Division for publication in the JOURNAL OF TRIBOLOGY. Manuscript received by the Tribology Division October 9, 1989; revised manuscript received May 22, 1990. Associate Editor: I. Green.

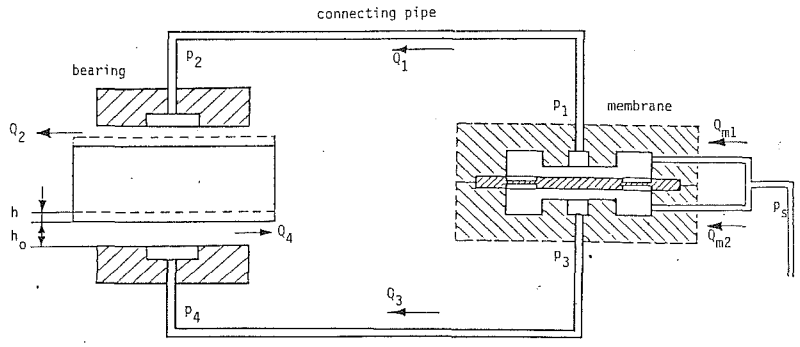

Fig. 1 Schematic of a membrane-compensated double-pad circular bearing

(1) The bearing system is modeled as a two-degree-of-freedom system with two lumped masses (Figs. 2 and 3).

(2) The pressure in the recess region is assumed to be constant while that in the annular region is governed by the Reynolds equation.

(3) The lubricant is incompressible and its viscosity and density are constant.

(4) Laminar flow exists in the bearing and in the membrane compensator.

(5) The ambient pressure is zero.

(6) The lubricant inertia force is neglected.

Mathematical Model

1 Governing Equations of Motion. A schematic of the double-pad externally pressurized bearing is shown in Fig. 1. The equation of motion of the bearing is given by (see Fig. 2)

$$M\ddot{h} = f_v + f(t) \tag{1}$$

where $f_v = f_{vb} - f_{vt}$ is the resultant pressure force of the two oil films acting on the bearing, and $f(t)$ is the externally applied load which is assumed to be composed of a static component and a sinusoidal component, i.e.,

$$f(t) = w_s + w_d \cos(\omega t) \tag{2}$$

Similarly, the equation of motion of the membrane is given by (Fig. 3)

$$m\ddot{x} + k_m x = f_m \tag{3}$$

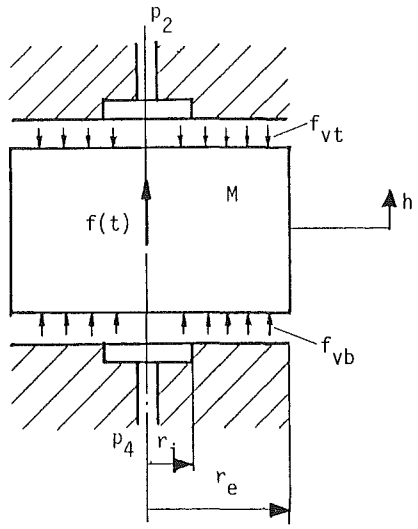

Fig. 2 Forces acting on the bearing element

where $f_m = f_{mb} - f_{mt}$ is the resultant pressure force acting on the membrane and k_m is the membrane stiffness. The membrane stiffness can be determined in terms of the material and geometry of the membrane element and is given by De Gast (1966) as

Nomenclature

$C_k = \dfrac{k_m x_0}{Mg}$ = dimensionless membrane stiffness

$C_p = \dfrac{\pi r_e^2 p_s}{Mg}$ = dimensionless supply pressure

$C_r = \dfrac{r_2}{r_e}$ = dimensionless radius parameter

$C_u = \dfrac{\pi^2 r_e^8 \mu^2}{M^2 g h_0^4 x_0}$ = dimensionless viscosity parameter

$C_w = \dfrac{R^4}{8Lh_0^3}$ = dimensionless geometry of the connecting pipe

$C_x = \dfrac{x_0}{h_0} = \left(\dfrac{\beta}{1-\beta}\dfrac{\ln R_1}{\ln R_i}\right)^{1/3}$

$C_z = m/M$ = ratio of membrane to bearing mass

E = modulus of elasticity of membrane, Pa

$f(t)$ = external load, N

$f_m = f_{mb} - f_{mt}$ = resultant pressure force acting on membrane, N

f_{mb}, f_{mt} = membrane pressure force, N

f_{mba}, f_{mta} = membrane annular region pressure force, N

f_{mbr}, f_{mtr} = membrane recess region pressure force, N

$f_v = f_{vb} - f_{vt}$ = resultant pressure force acting on bearing, N

f_{vb}, f_{vt} = bearing pressure force, N

f_{vba}, f_{vta} = bearing annular region pressure force, N

f_{vbr}, f_{vtr} = bearing recess region pressure force, N

$F_v = f_v/\pi r_e^2 p_s$ = dimensionless bearing pressure force

$F_m = f_m/\pi r_e^2 p_s$ = dimensionless membrane pressure force

g = gravitational constant, $g = 9.8$ m/s^2

h = bearing displacement, m

h_d = amplitude of bearing cyclic displacement, m

h_m = bearing mean displacement, m

h_0 = bearing film thickness at zero load, m

$H = h/h_0$ = dimensionless bearing displacement

$H_d = h_d/h_0$ = dimensionless amplitude of bearing cyclic displacement

$H_m = h_m/h_0$ = dimensionless bearing mean displacement

k_m = membrane stiffness, N/m

L = length of the connecting pipe, m

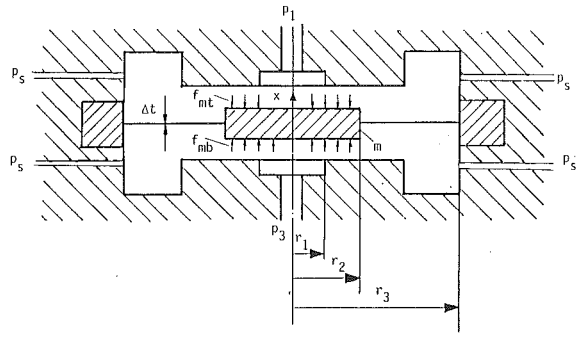

Fig. 3 Forces acting on the membrane

$$k_m = \frac{4\pi\Delta t^3 E}{3r_2^2(1-\lambda^2)} \frac{S^2-1}{(S^2-1)^2-4S^2(1nS)^2} \tag{4}$$

2 The Pressure Forces. The pressure forces in equations (1) and (3), depend on the bearing geometry, kinematic conditions, and the supply pressure. To obtain these pressure forces, the pressure distributions in the oil films must be first determined. The pressure forces in the recess region (f_{vtr}, f_{vbr}, f_{mtr}, f_{mbr}) are given by the recess areas multiplied by the corresponding recess pressures.

The pressure distribution in the annular region is governed by the Reynolds equation which is given, in cylindrical coordinates, by

$$\frac{n^3}{12\mu}\left(\frac{\partial^2 p}{\partial r^2} + \frac{1}{r}\frac{\partial p}{\partial r}\right) = V_2 - V_1 \tag{5}$$

Solving equation (5), for the pressure and then integrating over the annular area, the pressure forces in the annular regions of the bearing and membrane are obtained. For the top side of the bearing, the pressure force can be expressed as follows:

$$f_{vta} = \pi(r_e^2 - r_i^2)p_2 + \frac{\pi p_2}{\ln\left(\frac{r_i}{r_e}\right)}\left[r_e^2\left(\ln\left(\frac{r_e}{r_i}\right) - \frac{1}{2}\right) + \frac{1}{2}r_i^2\right]$$

$$-\frac{3\mu\pi\dot{h}}{(h_0-h)^3}\left\{\frac{r_e^2-r_i^2}{\ln\left(\frac{r_i}{r_e}\right)}\left[r_e^2\left(\ln\left(\frac{r_e}{r_i}\right) - \frac{1}{2}\right) + \frac{1}{2}r_i^2\right] + \frac{1}{2}(r_e^2-r_i^2)^2\right\} \tag{6}$$

For the bottom side of the bearing, the pressure force is given by:

$$f_{vba} = \pi(r_e^2 - r_i^2)p_4 + \frac{\pi p_4}{\ln\left(\frac{r_i}{r_e}\right)}\left[r_e^2\left(\ln\left(\frac{r_e}{r_i}\right) - \frac{1}{2}\right) + \frac{1}{2}r_i^2\right]$$

$$+\frac{3\mu\pi\dot{h}}{(h_0+h)^3}\left\{\frac{r_e^2-r_i^2}{\ln\left(\frac{r_i}{r_e}\right)}\left[r_e^2\left(\ln\left(\frac{r_e}{r_i}\right) - \frac{1}{2}\right) + \frac{1}{2}r_i^2\right] + \frac{1}{2}(r_e^2-r_i^2)^2\right\} \tag{7}$$

Similarly, for the top side of the membrane, the pressure force is given by

$$f_{mta} = \pi(r_2^2 - r_1^2)p_1 - \frac{\pi(p_s-p_1)}{\ln\left(\frac{r_1}{r_2}\right)}\left[r_2^2\left(\ln\left(\frac{r_2}{r_1}\right) - \frac{1}{2}\right) + \frac{1}{2}r_1^2\right]$$

$$-\frac{3\mu\pi\dot{x}}{(x_0-x)^3}\left\{\frac{r_2^2-r_1^2}{\ln\left(\frac{r_1}{r_2}\right)}\left[r_2^2\left(\ln\left(\frac{r_2}{r_1}\right) - \frac{1}{2}\right) + \frac{1}{2}r_1^2\right] + \frac{1}{2}(r_2^2-r_1^2)^2\right\} \tag{8}$$

Finally, for the bottom side of the membrane, the pressure force is given by

$$f_{mba} = \pi(r_2^2 - r_1^2)p_3 - \frac{\pi(p_s-p_3)}{\ln\left(\frac{r_1}{r_2}\right)}\left[r_2^2\left(\ln\left(\frac{r_2}{r_1}\right) - \frac{1}{2}\right) + \frac{1}{2}r_1^2\right]$$

Nomenclature (cont.)

m = equivalent membrane mass, Kg
M = bearing moving mass, Kg
n = general notation for film thickness, m
p_s = supply pressure, Pa
p_0 = bearing recess pressure at zero load, Pa
$p(r)$ = annular pressure, Pa
p_i = recess pressure in recess "i," Pa
$P_i = p_i/p_s$ = dimensionless recess pressure in recess "i"
Q_2, Q_4 = rate of lubricant flow out of the bearing, m^3/s
Q_1, Q_3 = rate of lubricant flow into the bearing, m^3/s
Q_{m1}, Q_{m2} = rate of lubricant flow into the membrane, m^3/s
r = radial coordinate direction, m
r_i, r_e, r_1, r_2, r_3 = radius (see Figs. 2 and 3), m
R = radius of the connecting pipe, m
$R_i = r_i/r_e$ = dimensionless radius of the bearing recess
$R_1 = r_1/r_2$ = dimensionless radius of the membrane recess
$S = r_3/r_2$ = membrane geometric parameter
Δt = membrane thickness, m
t = time, s
$T = \frac{p_s h_0^2}{\mu r_e^2} t$ = dimensionless time
V_1 = upward velocity of bottom surface, m/s
V_2 = upward velocity of top surface, m/s
w_s = static component of the external load, N
w_d = amplitude of cyclic component of the external load, N
$W_s = w_s/Mg$ = dimensionless static load
$W_d = w_d/Mg$ = dimensionless amplitude of cyclic load
x = membrane deflection, m
x_0 = membrane film thickness at zero load, m
$X = x/x_0$ = dimensionless membrane deflection
$\beta = p_0/p_s$ = pressure ratio
μ = lubricant viscosity, Pa-s
λ = Poisson's ratio
ω = excitation frequency, rad/s
$\Omega = \frac{\sqrt{C_u C_x}}{C_p}\sqrt{\frac{h_0}{g}}\,\omega$ = dimensionless excitation frequency

$$+\frac{3\mu\pi\dot{x}}{(x_0+x)^3}\left\{\frac{r_2^2-r_1^2}{\ln\left(\frac{r_1}{r_2}\right)}\left[r_2^2\left(\ln\left(\frac{r_2}{r_1}\right)-\frac{1}{2}\right)+\frac{1}{2}r_1^2\right]+\frac{1}{2}(r_2^2-r_1^2)^2\right\} \quad (9)$$

The total pressure forces at the top and bottom sides of the bearing are given, respectively, as

$$f_{vt}=f_{vtr}+f_{vta} \quad (10)$$

$$f_{vb}=f_{vbr}+f_{vba} \quad (11)$$

Similarly, the total pressure forces at the top and bottom sides of the membrane are given, respectively, as

$$f_{mt}=f_{mtr}+f_{mta} \quad (12)$$

$$f_{mb}=f_{mbr}+f_{mba} \quad (13)$$

The resultant pressure forces acting on the bearing and membrane are then given by

$$f_v=f_{vb}-f_{vt}$$

$$=\pi r_e^2(p_4-p_2)+\frac{\pi(p_4-p_2)}{\ln\left(\frac{r_i}{r_e}\right)}\left[r_e^2\left(\ln\left(\frac{r_e}{r_i}\right)-\frac{1}{2}\right)+\frac{r_i^2}{2}\right]$$

$$+\frac{3\mu\pi\dot{h}}{h_0^3}\left\{\frac{r_e^2-r_i^2}{\ln\left(\frac{r_i}{r_e}\right)}\left[r_e^2\left(\ln\left(\frac{r_e}{r_i}\right)-\frac{1}{2}\right)+\frac{r_i^2}{2}\right]+\frac{1}{2}(r_e^2-r_i^2)^2\right\}$$

$$\times\left[\frac{1}{\left(1+\frac{h}{h_0}\right)^3}+\frac{1}{\left(1-\frac{h}{h_0}\right)^3}\right] \quad (14)$$

$$f_m=f_{mb}-f_{mt}$$

$$=\pi r_2^2(p_3-p_1)+\frac{\pi(p_3-p_1)}{\ln\left(\frac{r_1}{r_2}\right)}\left[r_2^2\left(\ln\left(\frac{r_2}{r_1}\right)-\frac{1}{2}\right)+\frac{1}{2}r_1^2\right]$$

$$+\frac{3\mu\pi\dot{x}}{x_0^3}\left\{\frac{r_2^2-r_1^2}{\ln\left(\frac{r_1}{r_2}\right)}\left[r_2^2\left(\ln\left(\frac{r_2}{r_1}\right)-\frac{1}{2}\right)\right.\right.$$

$$\left.\left.+\frac{r_1^2}{2}\right]+\frac{1}{2}(r_2^2-r_1^2)^2\right\}\times\left[\frac{1}{\left(1+\frac{x}{x_0}\right)^3}+\frac{1}{\left(1-\frac{x}{x_0}\right)^3}\right] \quad (15)$$

The recess region pressures, p_1, p_2, p_3 and p_4, in equations (14) and (15), are related to the supply pressure (p_s), system geometry and kinematic conditions. These relations can be determined by the flow continuity in the system.

3 Continuity Equations. The continuity equation for the top side of the membrane is given by (Fig. 1)

$$Q_1=Q_{m1}+\pi r_2^2\dot{x} \quad (16)$$

and, for the bottom side of the membrane, it is given by

$$Q_3=Q_{m2}-\pi r_2^2\dot{x} \quad (17)$$

Similarly, the continuity equation for the top side of bearing is given by

$$Q_2=Q_1+\pi r_e^2\dot{h} \quad (18)$$

and, for the bottom side of the bearing, it is given by

$$Q_4=Q_3-\pi r_e^2\dot{h} \quad (19)$$

4 Lubricant Flow Rate.

Rates of flow into the membrane and out of the bearing

The rates of lubricant flow into the membrane and out of the bearing can be obtained from the equation governing the viscous, laminar flow between two parallel circular plates. This flow is given by

$$Q(r)=-\frac{\pi r n^3}{6\mu}\frac{\partial p}{\partial r} \quad (20)$$

Substituting $\partial p/\partial r$ from a solution of equation (5), the rate of flow out of the top side of the bearing is given by

$$Q_2=-\frac{\pi(h_0-h)^3}{6\mu}\left\{\frac{p_2}{\ln\left(\frac{r_i}{r_e}\right)}-\frac{3\mu\dot{h}}{(h_0-h)^3}\left[\frac{(r_e^2-r_i^2)}{\ln\left(\frac{r_i}{r_e}\right)}+2r_e^2\right]\right\} \quad (21)$$

and, out of the bottom of the bearing, given by

$$Q_4=-\frac{\pi(h_0+h)^3}{6\mu}\left\{\frac{p_4}{\ln\left(\frac{r_i}{r_e}\right)}+\frac{3\mu\dot{h}}{(h_0+h)^3}\left[\frac{(r_e^2-r_i^2)}{\ln\left(\frac{r_i}{r_e}\right)}+2r_e^2\right]\right\} \quad (22)$$

Similarly, the rate of flow into the top of the membrane is given by

$$Q_{m1}=\frac{\pi(x_0-x)^3}{6\mu}\left\{\frac{p_s-p_1}{\ln\left(\frac{r_2}{r_1}\right)}-\frac{3\mu\dot{x}}{(x_0-x)^3}\left[\frac{(r_2^2-r_1^2)}{\ln\left(\frac{r_1}{r_2}\right)}+2r_2^2\right]\right\} \quad (23)$$

and, into the bottom of the membrane, given by

$$Q_{m2}=\frac{\pi(x_0+x)^3}{6\mu}\left\{\frac{p_s-p_3}{\ln\left(\frac{r_2}{r_1}\right)}+\frac{3\mu\dot{x}}{(x_0+x)^3}\left[\frac{(r_2^2-r_1^2)}{\ln\left(\frac{r_1}{r_2}\right)}+2r_2^2\right]\right\} \quad (24)$$

Rate of flow into the bearing through the connecting pipe

Considering the laminar flow in the pipe connecting the top side of the membrane to the top side of the bearing, this flow is given by

$$Q_1=\frac{\pi R^4}{8\mu L}(p_1-p_2) \quad (25)$$

Similarly, for the pipe connecting the bottom side of the membrane to the bottom side of the bearing, the flow is given by

$$Q_3=\frac{\pi R^4}{8\mu L}(p_3-p_4) \quad (26)$$

Substituting equations (21) through (26) into equations (16) through (19), the equations of continuity become

$$\left[\frac{R^4}{8\mu L}+\frac{(x_0-x)^3}{6\mu \ln\left(\frac{r_2}{r_1}\right)}\right]p_1-\frac{R^4}{8\mu L}p_2=\frac{(x_0-x)^3p_s}{6\mu\ln\left(\frac{r_2}{r_1}\right)}$$
$$-\frac{\dot{x}}{2}\left[\frac{r_2^2-r_1^2}{\ln\left(\frac{r_1}{r_2}\right)}+2r_2^2\right]+r_2^2\dot{x} \quad (27)$$

$$\left[\frac{R^4}{8\mu L}+\frac{(x_0+x)^3}{6\mu \ln\left(\frac{r_2}{r_1}\right)}\right]p_3-\frac{R^4}{8\mu L}p_4=\frac{(x_0+x)^3p_s}{6\mu\ln\left(\frac{r_2}{r_1}\right)}$$
$$+\frac{\dot{x}}{2}\left[\frac{r_2^2-r_1^2}{\ln\left(\frac{r_1}{r_2}\right)}+2r_2^2\right]-r_2^2\dot{x} \quad (28)$$

$$\frac{R^4}{8\mu L}p_1+\left[\frac{(h_0-h)^3}{6\mu\ln\left(\frac{r_i}{r_e}\right)}-\frac{R^4}{8\mu L}\right]p_2$$
$$=\frac{\dot{h}}{2}\left[\frac{r_e^2-r_i^2}{\ln\left(\frac{r_i}{r_e}\right)}+2r_e^2\right]-r_e^2\dot{h} \quad (29)$$

$$\frac{R^4}{8\mu L}p_3+\left[\frac{(h_0+h)^3}{6\mu\ln\left(\frac{r_i}{r_e}\right)}-\frac{R^4}{8\mu L}\right]p_4$$
$$=-\frac{\dot{h}}{2}\left[\frac{r_e^2-r_i^2}{\ln\left(\frac{r_i}{r_e}\right)}+2r_e^2\right]+r_e^2\dot{h} \quad (30)$$

The continuity equations developed above can be used to solve for the recess region pressures, p_1, p_2, p_3 and p_4. These pressures, in a dimensionless form, are given by

$$P_1=\frac{0.5\,\dot{H}F+(C_w-C)\,P_2}{C_w} \quad (31)$$

$$P_2=\frac{C_w(A+\dot{X}DE)+0.5\,\dot{H}F(B-A)}{BC_w-(B-A)(C_w-C)} \quad (32)$$

$$P_3=\frac{(C_w-I)P_4-0.5\,\dot{H}F}{C_w} \quad (33)$$

$$P_4=\frac{C_w(G-\dot{X}DE)-0.5\,\dot{H}F(B-G)}{BC_w-(B-G)(C_w-I)} \quad (34)$$

where

$$A=(1-X)^3/[6\ln(R_1)]$$
$$B=C_w/C_x^3$$
$$C=(1-H)^3/[6\ln(R_i)]$$
$$D=(h_0r_2/x_0r_e)^2=(C_r/C_x)^2$$
$$E=(1-R_1^2)/[2\ln(R_1)]$$
$$F=(1-R_i^2)/(\ln R_i)$$
$$G=(1+X)^3/[6\ln(R_1)]$$
$$I=(1+H)^3/[6\ln(R_i)]$$

The governing equations (1) and (3), can also be rearranged into a dimensionless form as follows:

$$\ddot{H}=F_vC_{v1}+C_{v2}\cos(\Omega T)+C_{v3} \quad (35)$$

$$\ddot{X}=F_mC_{m2}-C_{m3}X \quad (36)$$

where

$$C_{v1}=\frac{C_uC_x}{C_p}$$

$$C_{v2}=\frac{C_uC_xW_d}{C_p^2}$$

$$C_{v3}=\frac{C_uC_xW_s}{C_p^2}$$

$$F_v=(P_4-P_2)+\frac{(P_4-P_2)}{\ln R_i}\left[\ln\left(\frac{1}{R_i}\right)-\frac{1}{2}+\frac{1}{2}R_i^2\right]$$
$$+3\dot{H}\left\{\frac{1-R_i^2}{\ln R_i}\left[\ln\left(\frac{1}{R_i}\right)-\frac{1}{2}+\frac{1}{2}R_i^2\right]\right.$$
$$\left.+\frac{1}{2}(1-R_i^2)^2\right\}\left[\frac{1}{(1+H)^3}+\frac{1}{(1-H)^3}\right]$$

$$C_{m2}=\frac{C_uC_r^2}{C_zC_p}$$

$$C_{m3}=\frac{C_uC_k}{C_zC_p^2}$$

$$F_m=(P_3-P_1)+\frac{(P_3-P_1)}{\ln R_1}\left[\ln\left(\frac{1}{R_1}\right)-\frac{1}{2}+\frac{1}{2}R_1^2\right]$$
$$+3\dot{X}\left(\frac{C_r}{C_x}\right)^2\left\{\frac{1-R_1^2}{\ln R_1}\left[\ln\left(\frac{1}{R_1}\right)-\frac{1}{2}+\frac{1}{2}R_1^2\right]\right.$$
$$\left.+\frac{1}{2}(1-R_1^2)^2\right\}\left[\frac{1}{(1+X)^3}+\frac{1}{(1-X)^3}\right]$$

By using the dimensionless recess pressures given by equations (31) through (34), equations (35) and (36) can be solved numerically to obtain bearing and membrane dynamics, respectively.

Results and Discussion

For all the results presented, the following dimensionless parameters are kept constant

$$C_z=0.0001,\quad C_w=10.0,\quad C_r=0.15,$$
$$R_1=0.33,\quad R_i=0.4,\quad C_u=244000$$

The choice of these constants is based on representative values that might be found in practice.

The nondimensional input parameters varied in this paper include membrane stiffness (C_k), supply pressure (C_p), pressure ratio (β), external load (W_s or W_d) and excitation frequency (Ω). The maximum nondimensional excitation frequency (Ω) considered in this research is one. For $\Omega > 1$, all results ap-

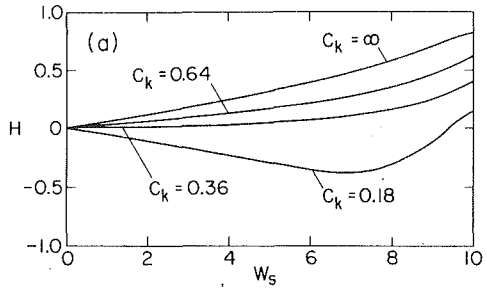

Fig. 4(*a*)

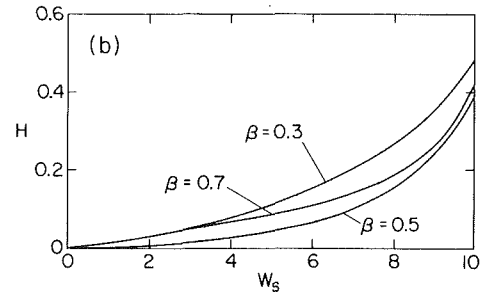

Fig. 4(*b*)

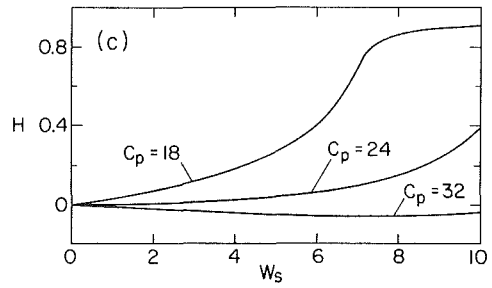

Fig. 4(*c*)

Fig. 4 Static displacement of bearing, (*a*) effects of C_k and W_s ($C_p = 24$, $\beta = 0.5$), (*b*) effects of β and W_s ($C_k = 0.36$, $C_p = 24$), (*c*) effects of C_p and W_s($C_k = 0.36$, $\beta = 0.5$)

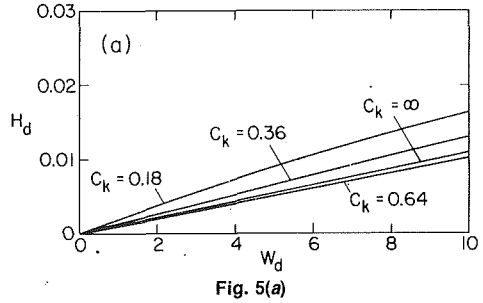

Fig. 5(*a*)

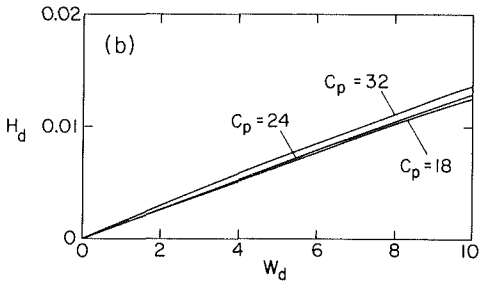

Fig. 5(*b*)

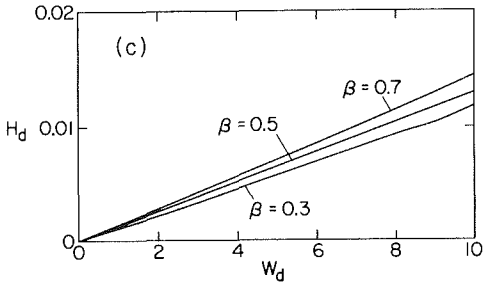

Fig. 5(*c*)

Fig. 5 Amplitude of cyclic displacement of bearing with zero mean load ($W_s = 0$, $\Omega = 1.0$), (*a*) effects of C_k and W_d ($C_p = 24$, $\beta = 0.5$), (*b*) effects of C_p and W_d ($C_k = 0.36$, $\beta = 0.5$), (*c*) effects of β and W_d($C_k = 0.36$, $C_p = 24$)

proach an asymptote and, therefore, no additional information is obtained. Considering some practical ranges for the variables which constitute Ω, the excitation frequency would vary from 1 to 7 cycles per second for the parameters considered and $\Omega = 1$. Under dynamic conditions, for the range of parameters considered, no cavitation occurred in the bearing or membrane. All results obtained are based on zero initial conditions.

1 Static Analysis. In the static analysis, the bearing is subjected to a constant external load. This analysis is presented so that comparisons can be made between the static and dynamic behaviors. Results from the static analysis are shown in Fig. 4. Figure 4(*a*) shows the variation of bearing displacement (H) with the static load (W_s) for various values of membrane stiffness (C_k). The results shown are for $C_p = 24$ and $\beta = 0.5$. When C_k approaches infinity, different operating conditions do not affect the motion of the membrane. Therefore, the system is equivalent to a capillary compensated bearing. Results obtained indicate that there exists an optimal value of C_k at which the stiffness of the bearing approaches infinity. This optimal value is found to be approximately 0.36. It is evident from the results that, as C_k assumes different values, the bearing can have positive, infinite and even negative stiffnesses (i.e., bearing displacement is opposite to the applied load). A negative stiffness can result in static instability (hammering) and fatigue failure of the diaphragm. Operating in the negative stiffness region, therefore, should be avoided. Results shown in Fig. 4(*a*) also indicate that, when the dimensionless load, W_s, exceeds 5.0, the system stiffness tends to decrease significantly, even with an optimal C_k.

The effects of pressure ratio on the bearing performance are shown in Fig. 4(*b*) for $C_k = 0.36$ and $C_p = 24$. For the given parameters, $\beta = 0.5$ seems to give the best performance. The system behavior, however, is relatively insensitive to the variation of β. Effects of supply pressure on the bearing performance are shown in Fig. 4(*c*) for $C_k = 0.36$ and $\beta = 0.5$. For a given load, the stiffness of the bearing increases with increasing C_p. If C_p is chosen large enough, the stiffness may approach infinity. However, too large a C_p can result in a bearing system having negative stiffness, and too small a C_p can result in a stiffness that is too low. Therefore, C_p should be carefully selected to achieve the best system behavior. These analytical results agree qualitatively with the analytical results obtained by De Gast (1966) and with the experimental results obtained by Row and O'Donoghue (1970).

2 Dynamic Analysis With Zero Mean Load. The dynamic characteristics of the bearing are first analyzed by comparing the response of the system under sinusoidal loading with the response under static loading. The results from this study are shown in Figs. 5 and 6. For a given amplitude of cyclic loading, and for $C_p = 24$, $\beta = 0.5$ and $\Omega = 1$, the amplitude of bearing displacement (Fig. 5(*a*)) is at least an order of magnitude smaller than the bearing displacement due to a static load of the same amplitude (Fig. 4(*a*)). Moreover, the value of C_k for which the system has an optimal response under static condition no longer produces an optimal response when $\Omega = 1.0$. In fact, the system

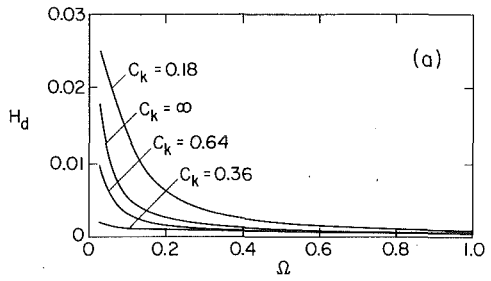

Fig. 6(*a*)

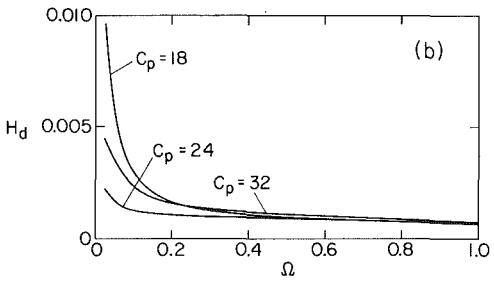

Fig. 6(*b*)

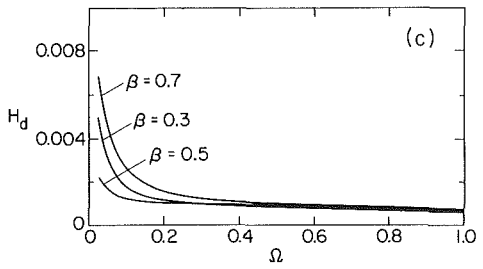

Fig. 6(*c*)

Fig. 6 Amplitude of cyclic displacement of bearing with zero mean load ($W_s = 0$, $W_d = 0.5$), (*a*) effects of C_k and Ω ($C_p = 24$, $\beta = 0.5$), (*b*) effects of C_p and Ω ($C_k = 0.36$, $\beta = 0.5$), (*c*) effects of β and Ω ($C_k = 0.36$, $C_p = 24$)

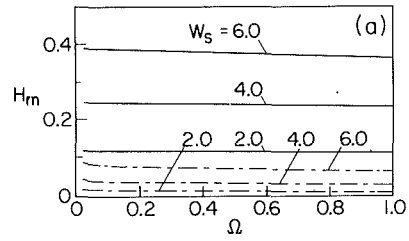

Fig. 7(*a*)

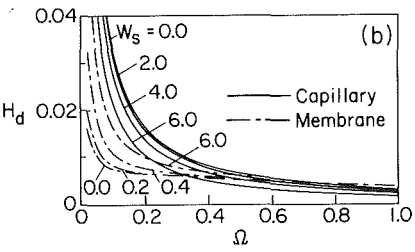

Fig. 7(*b*)

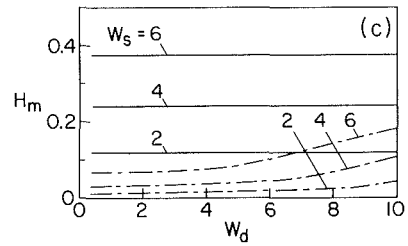

Fig. 7(*c*)

Fig. 7 Mean and cyclic displacement amplitudes of bearing with non-zero mean load for membrane ($C_k = 0.36$) and capillary ($C_k = \infty$) compensations ($\beta = 0.5$, $C_p = 24$), (*a*) effects of W_s and Ω ($W_d = 3.0$), (*b*) effects of W_s and Ω ($W_d = 3.0$), (*c*) effects of W_s and W_d (Ω = 0.5)

performance with capillary compensation (i.e., $C_k = \infty$) is almost as good as the best response with membrane compensation.

Figure 5(*b*) shows the amplitude of bearing displacement as a function of amplitude of excitation force for three values of C_p, again at an excitation frequency of $\Omega = 1.0$. The results presented are for $C_k = 0.36$ and $\beta = 0.5$. The system response is relatively insensitive to different values of C_p. The optimal value of C_p under these dynamic conditions is about 18 which is not the optimal value under static conditions. The amplitude of bearing displacement remains in a relatively small range (less than 0.014) for a wide range of amplitudes of excitation force. Thus, a smaller supply pressure can and should be used under dynamic conditions especially at higher frequencies.

Figure 5(*c*) shows the amplitude of bearing displacement as a function of the amplitude of excitation force for $C_k = 0.36$, $C_p = 24$ and three values of β. Again, the optimal value of β under dynamic conditions is not the optimal one found under static conditions, and the amplitude of bearing displacement is relatively insensitive to different values of β. The best response is obtained for $\beta = 0.3$.

The frequency response of the system is shown in Fig. 6 for $W_d = 0.5$. Figure 6(*a*) shows that the optimal value of C_k is 0.36 at low excitation frequencies (in the range of 0.0–0.4) for $C_p = 24$ and $\beta = 0.5$. As the excitation frequency goes beyond 0.4, the amplitude of bearing displacement for different values of C_k approaches approximately the same value. The curves shown in Figs 6(*b*) and 6(*c*) have almost the same trend as the curves shown in Fig. 6(*a*). The behavior of the system at low frequency (up to 0.4) is similar to that under a static loading. As the frequency increases, bearing displacements are very small for all values of C_k, C_p and β. This is due to the squeeze effect which dominates at the higher frequencies.

3 Dynamic Analysis With Non-Zero Mean Load. Since a cyclic load superimposed on a static load represents more common operating conditions, it is important to study the performance characteristics of the bearing when it is subjected to such loading. Under this loading condition, the response of the bearing is composed of a mean displacement H_m, and a cyclic displacement of amplitude H_d about H_m. For the following analysis, the values of C_p and β are taken as 24 and 0.5, respectively, and the dynamic excitation forces are assumed to be sinusoidal. Both a membrane compensated system with $C_k = 0.36$ and a capillary compensated system ($C_k = \infty$) are studied and the results are shown in Fig. 7. For $W_d = 3$, Fig. 7(*a*) shows the bearing mean displacement plotted against the excitation frequency for various values of static loads (W_s). For a given W_s, the results indicate that H_m is almost independent of the excitation frequency. The values of H_m for $C_k = \infty$ (capillary compensation) are much larger than those for $C_k = 0.36$ under the same operating condition. The amplitude of the bearing cyclic motion as a function of excitation frequency is shown in Fig. 7(*b*). The parameters are the same as those in Fig. 7(*a*). This motion is sensitive to the excitation frequency and to the static load only in the low frequency range. It becomes almost identical for all values of W_s when Ω is sufficiently high. Figure 7(*b*) indicates that H_d is practically independent of C_k at high frequencies. As expected, at low frequencies, H_d for capillary compensation is larger than that for membrane compensation. The effects of the amplitude of dynamic load (W_d) on the bearing mean displacement (H_m) are shown in Fig. 7(*c*) for $\Omega = 0.5$. For a given W_s, the analysis predicts that H_m is significantly affected only at the higher

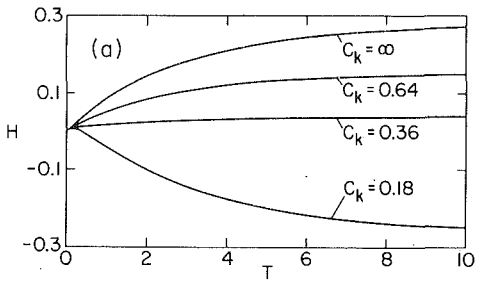

Fig. 8(*a*)

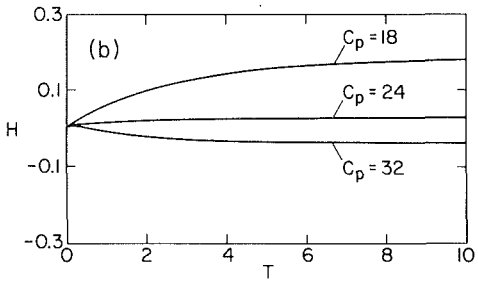

Fig. 8(*b*)

Fig. 8 Step response of bearing for $W_s = 0.4$ and $\beta = 0.5$, (*a*) effects of C_k ($C_p = 24$), (*b*) effects of C_p ($C_k = 0.36$)

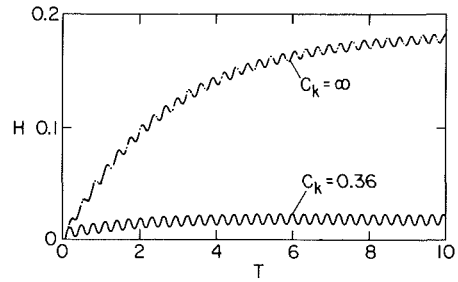

Fig. 9 Step-sinusoidal-input response of the bearing for membrane and capillary compensation ($C_p = 24$, $\beta = 0.5$, $W_s = 3.0$, $W_d = 4.0$ $\Omega = 1.0$)

values of W_s and W_d for membrane compensation. The bearing mean displacement with capillary compensation is significantly larger than that with membrane compensation and, for given W_s, it is independent of W_d.

4 Time Response Analysis. The transient analysis is conducted by looking at the time history of the bearing displacement when a static load or a dynamic load with nonzero mean value are applied. Figure 8(*a*) shows the transient response of the bearing displacement, H, when the bearing is subjected to a step load with $W_s = 4.0$, $\beta = 0.5$, and $C_p = 24$. The bearing with $C_k = 0.36$ has a much shorter settling time as well as a much smaller steady state displacement than the bearing with other C_k values. Thus, the system transient response seems to be very sensitive to the membrane stiffness. The effect of supply pressure (C_p) on the bearing time response is shown in Fig. 8(*b*) for $W_s = 4.0$, $\beta = 0.5$ and $C_k = 0.36$. The optimal value of C_p is 24 for the given values of C_k and β, and a long transient is experienced when the supply pressure is low. Data not shown indicate that the transient response is relatively insensitive to β.

Figure 9 shows the bearing transient response for $C_p = 24$, $\beta = 0.5$, $W_s = 3.0$, $W_d = 4.0$ and $\Omega = 1.0$. The transients are mainly due to the static step loading and is much larger in the capillary compensated bearing than in the membrane compensated bearing. The cyclic amplitude of the bearing with $C_k = \infty$ is smaller than that with $C_k = 0.36$.

Conclusion

In this paper, a circular, double-pad, externally pressurized thrust bearing compensated by a membrane restrictor or a capillary is studied. The response of the bearing is analyzed in detail under various static and dynamic loading conditions. Based on the results obtained, the following conclusions can be drawn:

1 Under static loading, the stiffness of the bearing can approach infinity for a relatively wide range of applied loads if the system parameters (C_k, C_p, β) are appropriately chosen. The system can also exhibit a negative stiffness when the membrane is too soft (i.e., small value of C_k) or when the supply pressure is too high.

2 The amplitude of the bearing displacement is generally an order of magnitude smaller under pure sinusoidal loading than under a static loading of the same amplitude. Moreover, the response of the bearing is relatively insensitive to different values of C_k, C_p and β when the excitation frequency is sufficiently high (i.e., $\Omega > 0.5$). This relative insensitivity is due to the dominance of the squeeze action at the higher frequencies. Therefore, a bearing with capillary compensation, which is much more inexpensive and less complicated than membrane compensation, can be used if the bearing is to be operated under sinusoidal, high-frequency conditions.

3 Under dynamic loading with a given nonzero mean (W_s), the mean displacement (H_m) of a membrane compensated bearing is relatively insensitive to the excitation frequency and is affected by the amplitude of cyclic loading (W_d) only when both W_d and W_s are relatively high. For both membrane and capillary compensations, the cyclic bearing displacement (H_d) is significantly affected by W_s only when the excitation frequency is relatively low. For a given W_s, H_m is significantly larger for capillary compensation than for membrane compensation.

4 The transient behavior of a membrane compensated bearing is generally better than that of a capillary compensated bearing, especially when a static loading component exists.

References

Brown, G. M., 1961, "Dynamics Characteristics of Hydrostatic Thrust Bearing," *Mach. Tool. Des. Res.*, Vols. 1-2 No. 1, p. 157.

Cusano, C., 1974, "Characteristics of Externally Pressurized Journal Bearing with Membrane-Type Variable-Flow Restrictors as Compensating Elements," *Inst. of Mechanical Engineers*, London, Vol. 188, No. 52, p. 527.

De Gast, J. G. C., 1966, "A New Type of Controlled Restrictor (M. D. R.) for Double Film Hydrostatic Bearing and Its Application to High-Precision Machine Tools," *Advances in Machine Tool Design and Research*, Pergamon Press, Oxford, p. 273.

Ghosh, M. K., and Majumdar, B. C., 1982, "Dynamic Stiffness and Damping Characteristics of Compensated Hydrostatic Thrust Bearing," *Journal of Lubrication Technology*, Trans. ASME, Vol. 104, No. 4, p. 491.

Licht, L., and Cooley, J. W., 1964, "Dynamics of Externally Pressurized Sliders with Incompressible and Compressible Film," ASME *Journal of Basic Engineering*, Trans., No. 2, Vol. 86, p. 396.

Mayer, J. E., and Shaw, M. C., 1963, "Characteristics of Externally Pressurized Bearing Having Variable External Flow Restrictors," ASME *Journal of Basic Engineering*, Vol. 85, p. 291.

O'Donoghue, J. D., and Rowe, W. B., 1969, "Compensation Methods for Externally Pressurized Bearings," *Engineer's Digest*, Vol. 30, No. 4, p. 49.

Optiz, H., Bottcher, R., and Effenberger, W., 1969, "Investigation on the Dynamic Behavior of Hydrostatic Spindle Bearing Systems," *Proc. 10th. Int. M. T. D. R. Conf.*, Pergamon Press, p. 453.

Rowe, W. B., and O'Donoghue J. P., 1970, "Diaphragm Valves for Controlling Opposed Pad Hydrostatic Bearing," *Proc. I. Mech. E.* Tribology Convention held at Brighton, paper 1.